Veterinary Integrative Sciences 2026; 24(1): e2026025-1-18. DOI: 10.12982/VIS.2026.025

Veterinary Integrative Sciences
ISSN: 2629-9968 (online)

Research article

In vitro differentiation of feline amniotic-derived mesenchymal stem cells into proximal tubular-like cells: A pilot study

Pachara Pornnimitara [1], Wanna Suriyasathaporn [1,4], Kantirat Yaja [2], Suteera Narakornsak [3,*] and Sasithorn Panasophonkul [1,4,*]

[1] Faculty of Veterinary Medicine, Chiang Mai University, Chiang Mai 50100, Thailand
[2] Clinical Research Center for Food and Herbal Product Trials and Development (CR-FAH), Faculty of Medicine, Chiang Mai University, Chiang Mai 50200, Thailand
[3] Department of Anatomy, Faculty of Medicine, Chiang Mai University, Chiang Mai 50200, Thailand
[4] Research Center of Producing and Development of Products and Innovations for Animal Health and Production, Chiang Mai University, Chiang Mai 50100, Thailand

Abstract

This study aims to isolate and characterize mesenchymal stem cells (MSCs) from the feline amniotic membrane and explore their potential for differentiation into proximal tubular-like cells (PTLCs) for regenerative medicine applications. The feline amniotic membrane-derived MSCs (AM-MSCs) from feline amniotic membranes were isolated successfully and characterized in terms of viability, morphology, and key MSC markers like CD73 and CD90. Exhibiting a shape reminiscent of fibroblasts, these cells also had a viability above 80% and could differentiate into adipogenic, chondrogenic, and osteogenic lineages after 21 days. Notably, the lack of hematopoietic indicators (CD34 and CD45) confirmed their mesenchymal lineage. The Differentiation into PTLCs was accomplished utilizing a protocol that incorporated Rho-Kinase (ROCK) inhibitor and specific growth factors, resulting in morphological alterations and gene expression reflective of PTLC characteristics. The upregulation of nephron-specific genes, such as Paired box gene 2 (*PAX2*), Gene Aquaporin 1 (*AQP1*), and Gamma-glutamyltransferase 1 (*GGT*), corroborated successful differentiation towards renal cell types, albeit with discrepancies among samples. These discoveries underscore the potential of feline AM-MSCs for the advancement of innovative therapeutic strategies for chronic kidney disease (CKD) in felines. Subsequent research should concentrate on refining differentiation protocols and undertaking *in vivo* assessments to ascertain their clinical efficacy in treating CKD and associated ailments in felines and potentially other species.

Keywords: Chronic kidney disease, Feline amniotic membrane, Mesenchymal stem cells, Proximal tubular-like cells, Regenerative medicine.

*Corresponding author:
Suteera Narakornsak, Department of Anatomy, Faculty of Medicine, Chiang Mai University, Chiang Mai 50200, Thailand. E-mail: suteera.n@cmu.ac.th.
Sasithorn Panasophonkul, Faculty of Veterinary Medicine, Chiang Mai University, Chiang Mai 50100, Thailand. E-mail: sasithorn.pana@cmu.ac.th.

Article history; *received manuscript: 23 January 2025, revised manuscript: 16 March 2025, accepted manuscript: 6 June 2025, published online: 17 June 2025,*
Academic editor; *Korakot Nganvongpanit*

INTRODUCTION

Chronic kidney disease (CKD) in felines is a progressive condition characterized by the gradual loss of kidney function over time, and it is a major cause of morbidity and mortality in aged cats (Aronson, 2016). The etiological factors that precipitate CKD are diverse, including variables such as the quantity of litter boxes available and the incidence of feline leukemia virus (FeLV) and feline immunodeficiency virus (FIV)(Piyarungsri et al., 2020). Many studies have found a strong relationship between CKD and acute kidney injury (AKI). AKI has been shown to accelerate the progression of CKD. Additionally, two factors associated with CKD decreased glomerular filtration rate and increased proteinuria are recognized as significant risk factors for AKI. Consequently, AKI inflicts substantial suffering, carrying a heightened risk of mortality or the development of long-term CKD in both humans and animals (Hsu and Hsu, 2016; Kim et al., 2019; Perini-Perera et al., 2021). Currently, managing and treating CKD presents considerable challenges, with renal transplantation being the only definitive treatment option for affected felines (Thornton, 2017).

Stem cell therapy is an innovative and emerging field of scientific research and clinical application with promising potential to treat various diseases in both veterinary and human medicine. Among the types of stem cells, mesenchymal stem cells (MSCs), are particularly intriguing due to their versatile properties, including anti-inflammatory, mitogenic, and immunomodulatory effects, as well as their ability to differentiate into various cell types (Westenfelder and Togel, 2011; Sobhani et al., 2017). One of the key advantages of MSCs is their abundant availability and minimal ethical constraints (Lukomska et al., 2019). These cells can be isolated from various adult tissues, such as bone marrow, adipose tissue, or heart (Hass et al., 2011; Westenfelder and Togel, 2011). In the pursuit of alternative sources of MSCs, researchers have turned their attention to the fetal membrane, which is readily accessible, abundant, and avoids ethical controversies. Various components of the fetal membrane, including the allantois fluid, amniotic fluid, amniotic membrane, and umbilical cord matrix, have been utilized for isolating MSCs in human (Hass et al., 2011), canine (Rashid et al., 2021), feline (Vidane et al., 2014), and murine models (Westenfelder and Togel, 2011). In felids, amniotic membrane derived-MSCs (AM-MSCs) appeared to be more readily obtainable and show a higher proliferation rate compared to other parts of the fetal membrane (Ambrosio et al., 2020). Moreover, their ability to differentiate into multiple cell types makes them attractive candidates for cell-based therapy, particularly in the context of treating kidney disease.

The proximal tubules play a critical role in maintaining kidney function, and their damage is a major factor in the progression of CKD in cats. Consequently, research into the potential of MSCs for regenerating damaged proximal tubules is ongoing. For example, a case report involving the intravenous injection of allogenic stem cells into a cat with CKD demonstrated clinical improvement, evidenced by enhanced clinical markers such as blood urea nitrogen (BUN) and creatinine (CREA) (Noh et al., 2021). Previous studies have highlighted the potential of stem cells for repairing and regenerating renal tissue, including proximal tubules, through their anti-inflammatory, immunomodulatory, and regenerative properties (Cianci et al., 2023). Additionally, previous studies have demonstrated renal proximal tubular-like cell (PTLC)differentiation in other species, including the co-culture of murine MSCs with proximal tubule cells, which led to the expression of renal-specific markers (Singaravelu and Padanilam, 2009). Furthermore, human-induced pluripotent stem cells have been successfully differentiated into PTLCs, exhibiting characteristic phenotypes and specific markers (Chandrasekaran et al., 2021). This study diverges to focus on the feline model, which is characterized by a notable deficiency in knowledge regarding renal cell line differentiation.

The study of proximal tubule cell differentiation in felines holds significant implications for both veterinary and human medicine. Advancing our understanding

of this process can provide critical insights into the pathophysiology of feline renal diseases. It also contributes to the development of innovative therapeutic strategies, including tissue engineering and cell-based therapies. By elucidating species-specific differences, identifying key signaling pathways, and examining the influence of feline-specific pathologies on differentiation mechanisms, this research can pave the way for more targeted and effective treatments.

Nevertheless, the existing body of knowledge pertaining to the differentiation capacity of feline MSCs into PTLCs remains insufficient, despite the crucial significance of PTLCs within the renal system due to their distinctive morphology and specialized functionalities. Our emphasis on PTLCs arises from their pivotal contribution to renal function and their potential as targets for therapeutic intervention. The advancement of cellular therapies for felines afflicted with renal disease necessitates several critical steps, including the validation of *in vitro* renal differentiation potency of feline MSCs, an exploration of the mechanisms underlying the differentiation of feline PTLCs, the standardization of feline PTLCs through the optimization of differentiation protocols aimed at preserving or enhancing quality, as well as conducting *in vivo* clinical trials in both autologous and allogeneic subjects encompassing both short-term and long-term assessments of safety and efficacy, ultimately progressing towards commercialization. Our focus on feline AMSCs was predicated on their accessible source and reduced immunogenic properties. This investigation concentrated on the preliminary phase of cell therapy development, specifically the *in vitro* renal differentiation potency of feline MSCs and the mechanisms governing PTLC differentiation.

MATERIALS AND METHODS

This study was conducted with informed consent obtained from the animal owners and was approved by the Animal Care and Use Committee of the Faculty of Veterinary Medicine, Chiang Mai University (FVM-ACUC), on March 19, 2021 (Approval No. S8/2564)

Animals and sample collection

The fetal amniotic membranes were collected through cesarean section from three full-term, healthy pregnant queens. Queen No.1 provided 3 amniotic tissues, Queen No. 2 provided 6 amniotic tissues, and Queen No. 3 provided 5 amniotic tissues. All participating pregnant queens were screened for feline leukemia virus (FeLV) and feline immunodeficiency virus (FIV) using a Bionote Rapid FIV Ab/FeLV Ag Feline Test Kit (Bionote USA, Big Lake, USA), which detects FIV antibodies and FeLV antigens, and only those with confirmed negative results were included in the study. Following the cesarean section, the fetal amniotic tissues, connected to allantoid sac, were washed with sterile phosphate-buffered saline (PBS) (Amresco®, Ohio, USA) to remove blood clots. The tissues were then stored in a sterile glass bottle containing PBS with 1% Penicillin-Streptomycin (P/S) (Gibco, USA) and transported to the laboratory within 2 hours to prevent necrosis and preserve their quality.

Isolation and cultivation

In the laboratory, the amniotic membrane (AM) was mechanically separated from the allantoid sac and then washed repeatedly with sterile PBS to remove debris and blood. The isolation of feline AM-MSCs was conducted using the method described by Vidane et al. (2016), with minor modifications. The fetal AM from each queen were combined and digested with 0.25% trypsin-EDTA (Gibco®, Life technologies, USA) at 37°C for 30 min, and then rinsed 3 times with PBS. The digested AM was minced into 1-2 mm^3 and incubated in 2 mg/ml collagenase type 1 (Gibco®, Life technologies, USA) at 37°C for 1 hour. The isolated cells were filtered through 75 µm cell strainer and centrifuged at 1,500 *g* for 5 min. The cell

pellet was resuspended in MSC medium consisting of high-glucose Dulbecco's modified Eagle medium (DMEM) (Gibco®, Life technologies, USA) with 10% fetal bovine serum (FBS) (Thermo Fisher Scientific, Massachusetts, USA) and 1% P/S. The cells were then cultured in a 25 cm^2 tissue culture flask (Corning Incorporated, NY, USA) in humidified incubator at 37°C with 5% CO_2 and saturated humidity. After 24 hours, non-adherent cells were removed, and the medium was changed every 3 days. The cells were trypsinized upon reaching 80% confluence, expanded in a 25 cm^2 tissue culture flask, cultured at the same condition (passage 1). The cells were frozen in DMEM supplemented with 20% FBS and 10% dimethyl sulfoxide (DMSO) (Sigma-Aldrich, St. Louis, MO, USA) at -80°C for 24 hours using a freezing container, then cryopreserved in liquid nitrogen. To attain a certain degree of cell-type enrichment, a screening framework based on the established traits of MSCs, including plastic adherence and proliferative potential, was instituted, followed by a series of subculturing procedures. The AM-MSCs at the 3rd passage were utilized to assess the stemness characteristics of AM-MSCs, including morphology, plastic adherence, proliferation potency, expression of cell surface markers, trilineage differentiation potentials, and differentiation potency with renal proximal tubule cells.

MSC Characterization

Alarmar Blue proliferation assay

Alamar Blue assay quantifies cell proliferation through redox-based conversion of resazurin to resorufin. This metabolic reduction, performed by viable cells, causes a colorimetric shift measurable at 540-630 nm. Initially, cells were seeded at a density of $2x10^3$ cells/well in 24-well plates and cultured in MSC medium for 24 hours. Following this, the medium was removed, and 100 µl of 10% alamar blue (Sigma-Aldrich,USA) in DMEM was added to the cells. They were then incubated at 37°C, 5% CO_2 with 95% humidity for 4 hours. Afterward, supernatant liquid samples were transferred into 96-well plates for absorbance evaluation, utilizing the colorimetric change of each well. Subsequently, the cells in 24-well plates were replenished with MSC medium and continuously cultivated under the same conditions. Resorufin absorbance was measured at 48-hour intervals over a 21-day period using a spectrophotometric microplate reader (Original Multiskan EK, Thermoscientific, UK). Samples consisting of 10% alamar blue solution unexposed to cells were used as a control.

Flow cytometry

The AM-MSCs were trypsinized and centrifuged to obtain a cell pellet (totalling $1x10^6$ cells). The cells were then divided into 1.5 ml microcentrifuge tubes and centrifuged at 1,500 *g* for 5 min. The pellet was washed twice in PBS containing 0.2%FBS, and then the cell was resuspended in 50 µl PBS with 2% bovine serum albumin (2%BSA-PBS) incubate on ice for 30 min. The cells were probed with fluorescent-conjugated antibodies as follows: CD34 (FITC mouse anti-human CD34; BD Pharmingen), CD45 (FITC mouse anti-human CD45; BD Pharmingen), CD44 (PE anti-mouse/human CD44; Bio-Legend), CD73 (Immuno Tools GmbH, Friesoythe, Germany), CD90 (PE mouse anti-human CD90; BD Pharmingen), and CD105 (mouse anti-human CD105; BIO-RAD), HLA-ABC (Immuno Tools GmbH, Friesoythe, Germany), and HLA-DR (antibody clone: TÜ39; BD Biosciences). Fluorescent-conjugated mouse isotype controls were used as negative controls (FITC mouse isotype control, PE mouse isotype control, APC mouse isotype control; Biolegend,San Diego,USA). Cell fluorescence was analysed using a DxFLEX Flow Cytometer (Beckman Coulter, USA) and further processed with Cytexpert for DxFLEX software (Beckman Coulter, USA).

Trilineage differentiation

On pre-differentiation, 80% confluent AM-MSCs of passage 3 (P3) were harvested with 0.25% trypsin-EDTA and centrifuged at 1,500 *g* for 5 min. After removing the supernatant, the pellet was resuspended in MSC medium and seeded into 24-well plates at a density of 5×10^4 cells/well. The cells were cultured until reaching 80% confluence, after which they were subjected to differentiation potential assays for adipocytes, chondrocytes, and osteocytes.

Adipogenic differentiation

To initiate adipogenic differentiation, the MSC medium in the 24-well plate culturing AM-MSCs was replaced with adipogenic medium [MSC medium supplemented with dexamethasone (10^{-6} mol, Sigma-Aldrich, USA) , insulin (5 µg/ml, Sigma-Aldrich, USA) , and indomethacin (60 µmol, Sigma-Aldrich, USA)] and cultured for 3 weeks at 37 °C under 5% CO_2 and saturated humidity, with media replacement every 3 days. The adipogenic phenotype was confirmed using Oil-red O staining (Sigma-Aldrich, USA), which stains lipids in adipocytes red.

Chondrogenic differentiation

For chondrogenic differentiation, the AM-MSCs were exposed to chondrogenic medium, which consisted of MSC medium supplemented with dexamethasone (0.1 µmol/L), insulin (10 µg/ml) and ascorbic acid (50 µg/ml, Sigma-Aldrich, USA) and cultured at 37 °C under 5% CO_2 and saturated humidity, with media replacement every 3 days. After 21 days, the chondrogenic phenotype was verified using safranin O staining (Sigma-Aldrich, USA). Safranin O stains cartilage and mucin orange to red, while nuclei are stained black, with staining intensity correlating with proteoglycan content in the extracellular matrix of cartilage.

Osteogenic differentiation

The osteogenic differentiation was induced by culturing AM-MSC in osteogenic medium, which consisted of MSC medium supplemented with dexamethasone (0.1 µmol/L), β-glycerol phosphate (10 mM, Sigma-Aldrich, Steinheim, Germany) and ascorbic acid (50 µg/ml). The cells were cultured at 37 °C under 5% CO2 and saturated humidity, with media replacement every 3–4 days. At 21 days of culture, differentiation was evaluated by staining with Alizarin Red S, which binds to calcium deposits, that appear orange to red. These deposits are indicative of osteocyte formation and are commonly used as a marker for osteogenic differentiation. AM-MSCs cultured in MSC medium served as controls for normal condition.

Renal proximal tubule-like cell (PTLC) differentiation

At 80% confluence, AM-MSCs at P3 were harvested using 0.25% trypsin-EDTA and centrifuged at 1,500 *g* for 5 min. After removing the supernatant, the pellet was resuspended in MSC medium, seeded at a density of 2×10^4 cells/well in 24-well plates, and incubated at 37°C under 5% CO_2 and saturated humidity. The following day, the medium was replaced with DMEM containing ROCK-inhibitor (10 µmol/ml, Merk Millipore, Germany) and incubated under the same conditions. After 24 hours, the medium was switched to PTLC medium, which consisted of MSC medium supplemented with bone morphogenetic protein 2 (10 ng/ml, BMP2) (Merk Millipore, Germany), bone morphogenetic protein 7 (2.5 ng/ml, BMP7) (Merk Millipore, Germany), transforming growth factor beta (0.5 ng/ml, TGF-β) (Merk Millipore, Germany), and insulin (5 µg/ml). The differentiated cells were incubated under the same conditions, with the medium changed every other day for 21 days. The AM-MSCs cultured in MSC medium were used as controls for normal conditions. Analysis was performed using hematoxylin and eosin staining for morphology and real-time quantitative polymerase chain reaction (RT-qPCR) for gene expression.

Hematoxylin and eosin staining

After 21 days, both the differentiated cells and control cells were fixed with 4% paraformaldehyde at 4°C for 4 hours and then stored in PBS at 4°C. Hematoxylin and eosin staining were performed as follows: the cells were washed twice with purified water and stained with hematoxylin for 6 min. After washing, the cells were dehydrated with 80% ethanol for 2 minutes. Next, the cells were stained with eosin for 5 min, followed by two washed with 95% ethanol and 100% ethanol, respectively, for 2 min each. Finally, the cells were air-dried, and the morphology of PTLCs was observed under a light microscope.

Real-time quantitative polymerase chain reaction (RT-qPCR)

After 14 and 21 days, total RNA extraction was performed using an Illustra™ RNAspin Mini RNA Isolation Kit (GE Healthcare, UK), following the manufacturer's instructions. RNA concentration was measured using a Nanodrop spectrophotometer (Nanodrop Technologies, Montchanin, USA) and the RNA was reverse transcribed into cDNA using a Tetro™ cDNA Synthesis Kit (Bioline, USA) according to the manufacturer's instructions. For RT-qPCR protocol, 8 of µl of cDNA template was prepared by adding 2 µl of mixed reverse and forward target primers and 10 µl of SYBR Green PCR Master Mix (Invitrogen, Thermo Fisher Scientific, Massachusetts, USA) Real-time quantitative polymerase chain reactions were performed using the ABI 7500 Fast Real-Time PCR System (Applied Biosystems™, USA) with temperature cycling. *GAPDH* was used as an internal control. The RT-qPCR was performed in triplicates. Relative expression levels for each primer set were normalized to the expression of *GAPDH* using the $2^{-\Delta\Delta CT}$ method (Livak and Schmittgen, 2001). Determination of cell differentiation into renal proximal tubule-like cell and the expression of phenotype-related genes, specifically *PAX2*, *AQP1* and *GGT*, were measured. The data were presented as the expression level relative to the corresponding date in control group. Primers used in this study are shown in Table 1.

Table 1 Real-time PCR primer sequences.

Gene	Sequence		Accession No.
PAX2	Forward 5'-3'	GACTATGTTCGCCTGGGAGATTC	XM_047826479
	Reverse 5'-3'	AAGGCTGCTGAACTTTGGTCCG	
AQP1	Forward 5'-3'	CTTGCCATTGGCTTGTCTGTGG	NM_198098
	Reverse 5'-3'	CCAGTGGTTTGAGAAGTTGCGG	
GGT	Forward 5'-3'	TGACGTACCACCGCATCGTAGA	XM_019814705
	Reverse 5'-3'	CAGCGAAGAACTCGGAGGTCAT	
GAPDH	Forward 5'-3'	GCCGTGGAATTTGCCGT	XM_006933438
	Reverse 5'-3'	GCCATCAATGACCCCTTCAT	

Statistical analysis

The data on MSCs proliferation potential, cell surface markers expression, and PTLC-related genes expression were presented as mean ± standard error of mean (SEM). Differences in proliferation rates of AM-MSCs at different time points were assessed using a linear mixed model (PROC MIXED, SAS), with statistically defined as $p < 0.05$. Flow cytometry results were analyzed descriptively to characterize surface maker expression. For the PTLC differentiation process, gene expression level was evaluated descriptively, comparisons between control and differentiated groups, as well as between day 14 and day 21, were performed using the non-parametric Mann-Whitney U test (GraphPad Prism version 5.01, GraphPad Prism software, Inc., CA, USA).

RESULTS

Feline amniotic-derived mesenchymal stem cell isolation

In this study, feline AM-MSCs were successfully isolated from all caesarian-delivered cats. The yield of isolated cells was 0.95×10^6 cells/g of amniotic tissue, with an average cell viability of 89%. Within 24 h of initial plating, most isolated cells adhered to the culture surface, forming a heterogeneous monolayer after 48 h. These heterogeneous populations exhibited two distinct cell morphologies: fibroblast-like cells with elongated shapes, arranged in clusters of 5-10 cells, and polygonal epithelial-like cells predominantly located at the borders of the fibroblast-like clusters (Figure 1A). During sub-cultivation, the epithelial-like cells decreased dramatically with each passage, resulting in a heterogeneous population predominantly composed of fibroblast-like cells. These fibroblast-like cells persisted in high numbers through subsequent passages, while epithelial-like cells became rarely observed. The cultures consistently reached confluence within 14 days (Figure 1B-C).

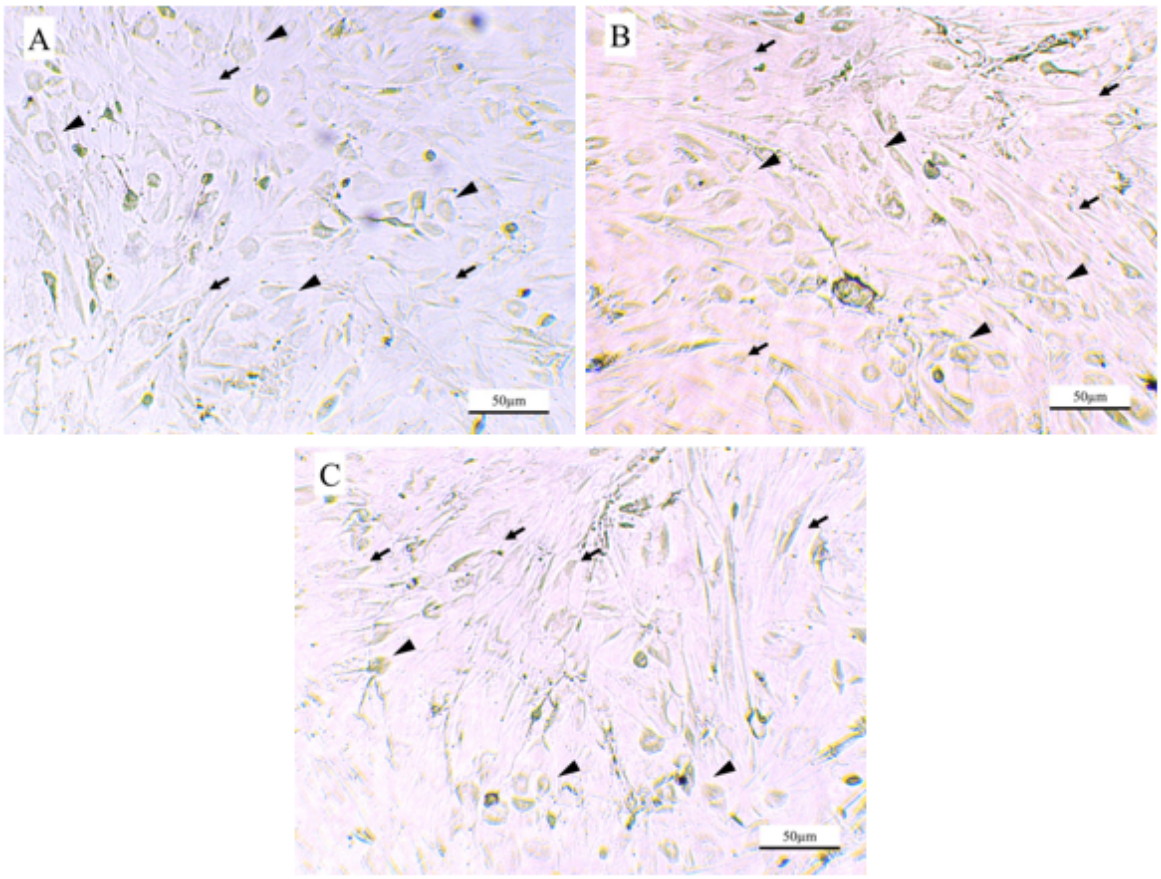

Figure 1 Morphological characteristics of feline AM-MSCs during primary culture. (A) On day 7 post-isolation, the heterogenous cell population displayed two distinct morphologies: elongated, fibroblast-like cells (arrowhead) and polygonal, epithelial-like cells (arrow). (B) On day 14, a heterogeneous population with the characteristic spindle-shaped, fibroblast-like morphology typical of MSCs infiltrated with epithelial-like cells was observed. (C) By day 21, fibroblast-like cells proliferated and expanded their cytoplasm, while epithelial-like cells become rare. Scale bar = 50 μm.

Cell proliferation analysis by Alamar Blue assay

The proliferation potential of all isolated AM-MSCs, assessed using the Alamar Blue assay, exhibited a typical biphasic growth pattern. AM-MSCs at P3 began proliferating early in the cultivation period. Viability increased significantly between days 1, 3 and 5, rising from 21.4 ± 0.85%, 27.3 ± 2.7% and 32.9 ± 1.93%, respectively, and exhibited a period of constant exponential growth until days 13 of culture. However, it was observed that between days 5 and 7, cell proliferation slightly decreased to 27.8 ± 0.89% during the log phase, and then the cell number increased progressively. By day 13, the cell population had increased from 28.9 ± 0.38% to 35 ± 0.12%, after which the growth rate proceeded slowly until day 19 and gradually declined on day 21 (Figure 2). Throughout the cultivation period, MSC viability increased significantly at an average growth rate of 1.2-fold every 2 days, particularly on days 3, 5, and 11.

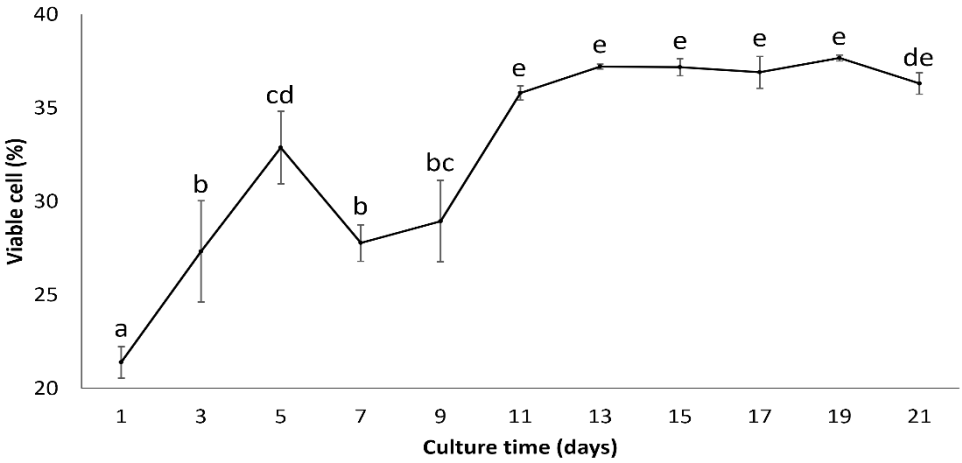

Figure 2 The growth curve of feline AM-MSCs at passage 3 during 21 days of culture demonstrates significant early proliferation, with marked increases in viability on days 1, 3, and 5. The cells underwent exponential growth until day 13, despite a brief decline in proliferation between days 5 and 7. This high level of cell proliferation continued until day 19, after which the cell number gradually decreased. The growth curve was plotted with mean ± SEM of viable cell and different letters indicate statistically significant differences (P≤0.05).

Expression of mesenchymal stem cell biomarker

Flow cytometry analysis of AM-MSCs at passage 3 (n=3) revealed positive expression of key MSC markers. CD90 was expressed at consistently high levels (80 ± 1.1%), while CD73 showed moderate expression (40.8 ± 9.7%). Additionally, low-level expression of MHC class I (HLA-ABC) was detected (5.6 ± 3.3%), whereas hematopoietic markers (CD34 and CD45) and MHC class II (HLA-DR) were undetectable (Figure 3). The variability in CD73 expression among individual samples was notable, ranging from 21.6 to 53.1%, while CD90 expression remained consistent across all samples (78.7 to 82.2%).

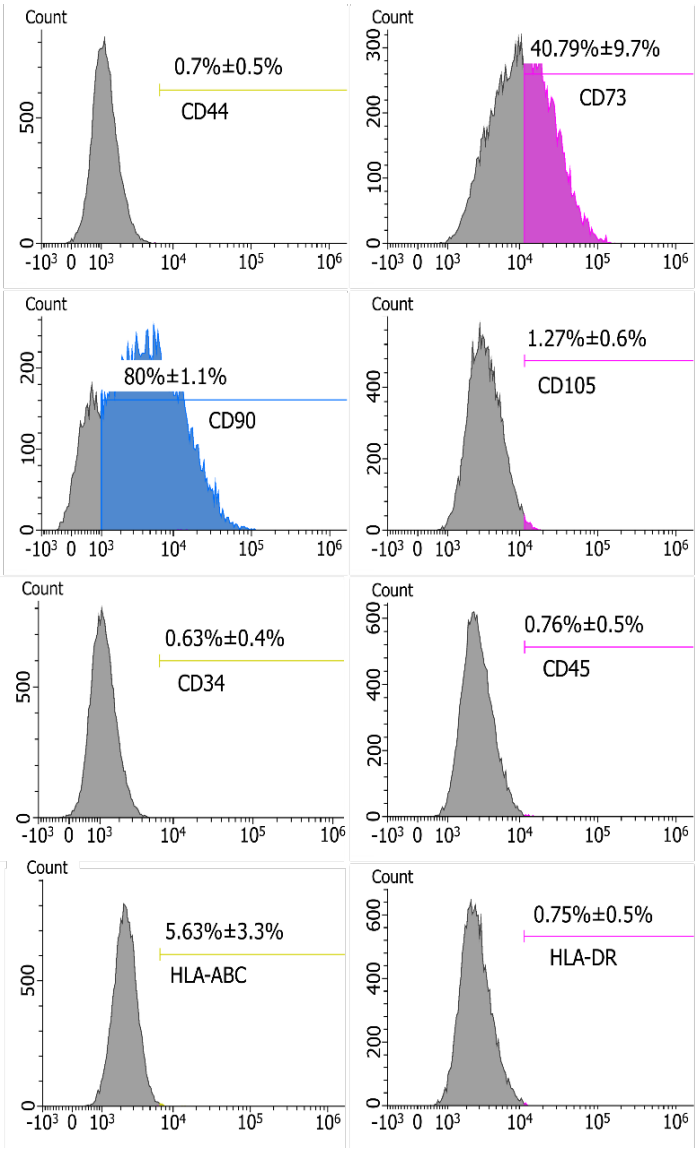

Figure 3 Flow cytometry analysis demonstrating the expression of mesenchymal stem cell (MSC) surface markers in feline amnion-derived MSCs (AM-MSCs) at passage 3 (n = 3). Approximately 80% of AM-MSCs were positive for CD90, while more than 40% expressed CD73. In contrast, hematopoietic markers (CD34 and CD45) and human leukocyte antigen (HLA)-DR were not detected. A low level of human leukocyte antigen (HLA)-ABC expression was observed. Data are presented as the mean percentage of marker-positive cells ± standard error of the mean (SEM). Abbreviations: FITC, fluorescein isothiocyanate; PE, phycoerythrin; APC, allophycocyanin.

The attributes of trilineage differentiation

The trilineage differentiation potential of AM-MSCs was thoroughly evaluated using specific induction protocols for adipogenic, chondrogenic, and osteogenic lineages. After 21 days of culture, adipogenic differentiation was confirmed by the presence of intracellular lipid droplets, which were positively stained with Oil red O (Figure 4A-B). The differentiated cells predominantly exhibited a stellate morphology, characterized by polygonal cytoplasm surrounding the nucleus, and elongated, shrunken organelles situated at the cytoplasmic corners. Additionally, droplet-like organelles were observed in the central cytoplasmic region of the differentiated cells. In the case of chondrogenic differentiation, strong positive staining with Safranin O indicated a high proteoglycan content (Figure 4D-E).

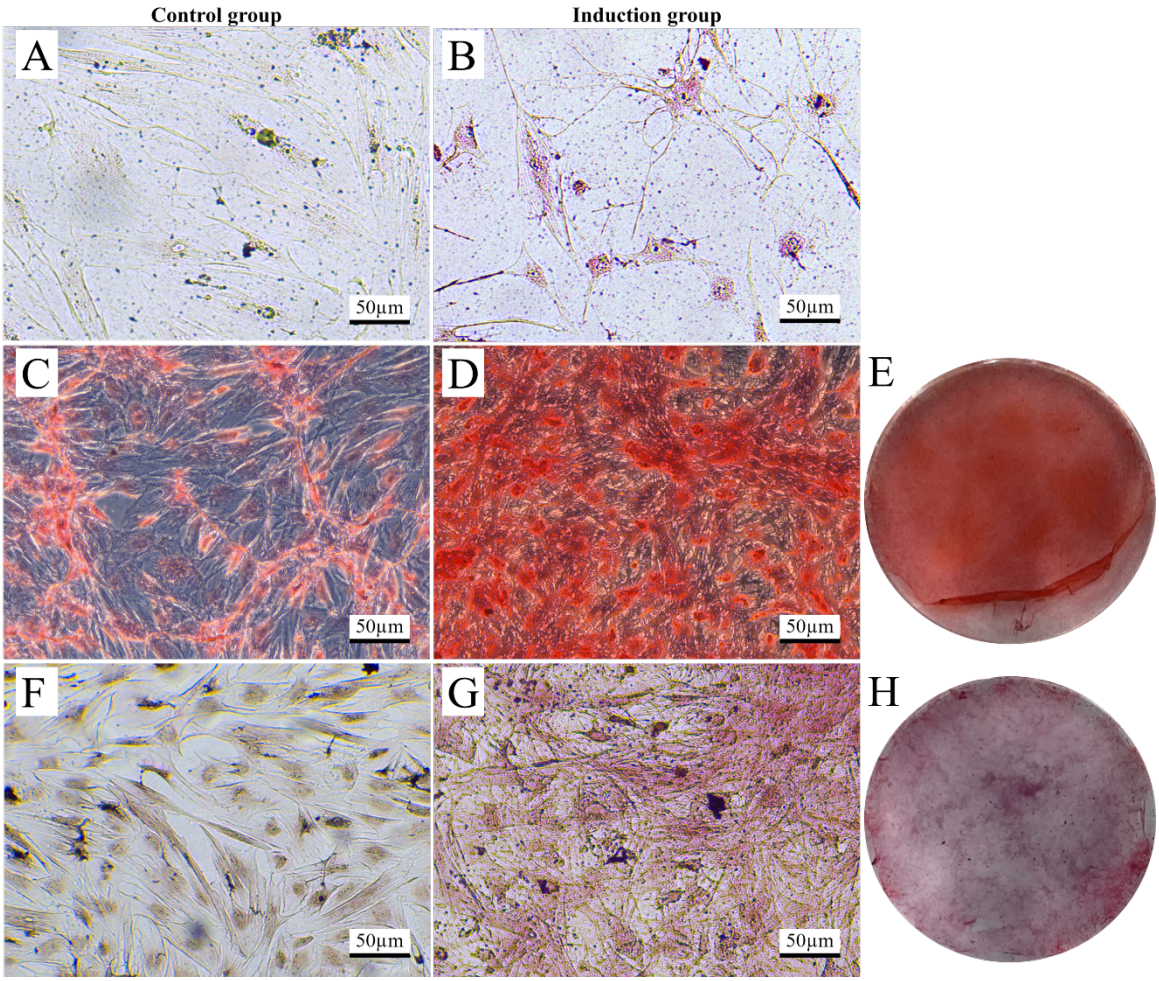

Figure 4 Trilineage differentiation potential of feline amnion-derived mesenchymal stem cells at passage 3. After 21 days of culture, feline AM-MSCs exhibited adipogenic, chondrogenic, and osteogenic differentiation (B, D-E, and G-H) compared to controls (A, C, and F). Adipocytes showed positive Oil Red O staining, indicating the presence of intracellular lipid droplets (B). Chondrocytes exhibited positive Safranin O staining, highlighting the presence of cartilage extracellular matrix (D-E). Osteocytes were positively stained with Alizarin Red S, indicating the presence of calcium deposits (G-H). Both chondrogenic (E) and osteogenic (H) differentiation showed strong staining in top-down views. Scale bar = 50 μm.

Differentiated cells were detected after 15 days in chondrogenic medium, with a higher concentration than the undifferentiated control group. The differentiated cells were densely packed, with overlapping patterns observed in high-concentration areas. Morphologically, these cells predominantly exhibited a spindle shape with elongated cytoplasm and centrally positioned nuclei. Intense red staining was noted in the nuclei, with mild red staining in the cytoplasm. Notably, in the culture plate of the chondrogenic group (Figure 4E), Safranin O staining revealed large, rounded red-stained clusters scattered throughout the culture surface. Osteogenic differentiation was demonstrated by Alizarin Red S staining, which remarkably revealed red dye binding to calcium deposits in the induced cells (Figure 4G-H). Differentiated cells became detectable after 12 days of culture in osteogenic medium. In regions of high cell concentration, densely packed cells were observed with overlapping features, primarily exhibiting polygonal morphology and elongated cytoplasmic extensions at the periphery. In the osteogenic group culture plate (Figure 4H), Alizarin Red S staining showed

numerous small, intense, red-stained clusters indicative of localized calcium deposition.

Renal proximal tubule-like cells (PTLCs) differentiation

Morphological observation

The morphology of feline AM-MSCs differentiated into renal proximal tubule-like cells was observed under a light microscope during 21 days of culture period, both with and without hematoxylin and eosin (H&E) staining (Figure 5 and 6). By day 7, the morphology of induced AM-MSCs initially changed from a spindle-shaped fibroblast-like appearance to a polygonal shape which is a characteristic of epithelial cells (Figure 5B). The number of expanded polygonal-shaped cells gradually increased over time, while fibroblast-like cells of AM-MSCs decreased markedly throughout the differentiation period (Figure 5B, 5C, and 5D). By day 21, under the differentiated circumstance, the cultivated feline AM-MSCs were predominantly composed of the expanded polygonal-shaped cells, exhibiting specific characteristics: larger, densely packed nuclei, and abundant cytoplasm elongated, which appeared prominently under H&E staining (Figure 6A and 6C) when compared with control group (Figure 6B and 6D).

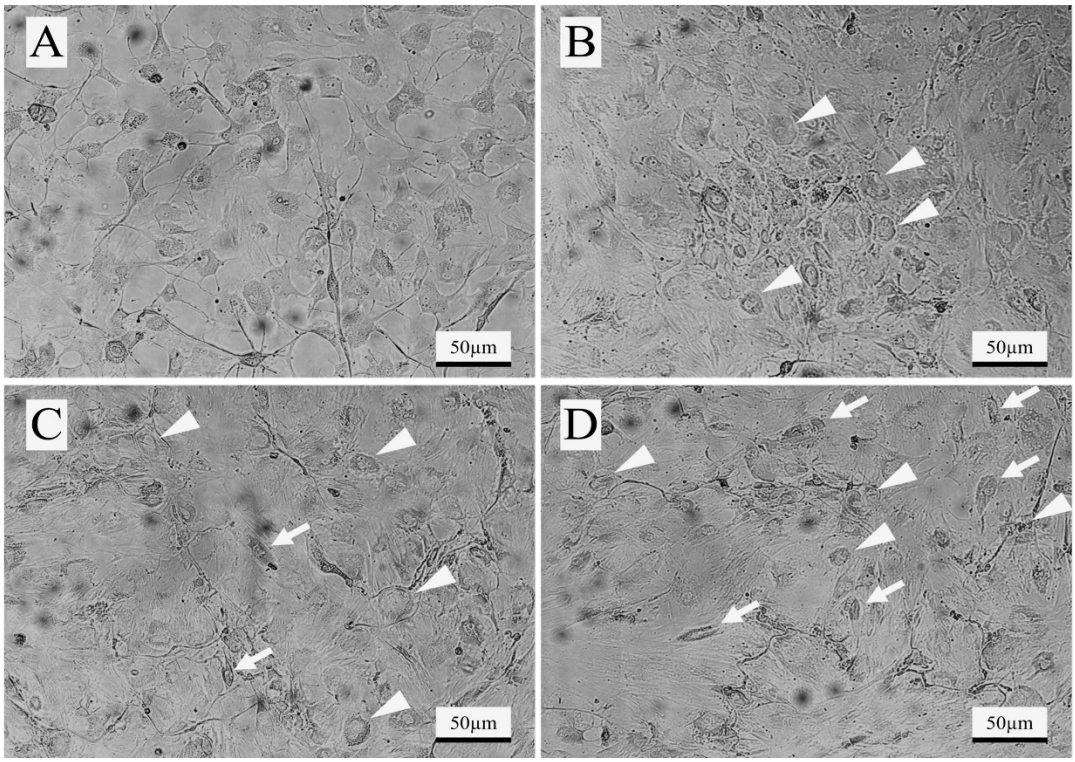

Figure 5 Morphological changes of feline AM-MSCs during differentiation into PTLCs. Day 0 or after treat with rock-inhibitor: (A) Cells displayed polygonal shapes and neuron-like morphology. Day 7: (B) Polygonal-shaped cells contracted together (arrowhead) with lower contribution. Day 14(C) and 21(D): Cells became more contracted left expanded and elongated(arrow) at low density area. Scale bar = 50 μm.

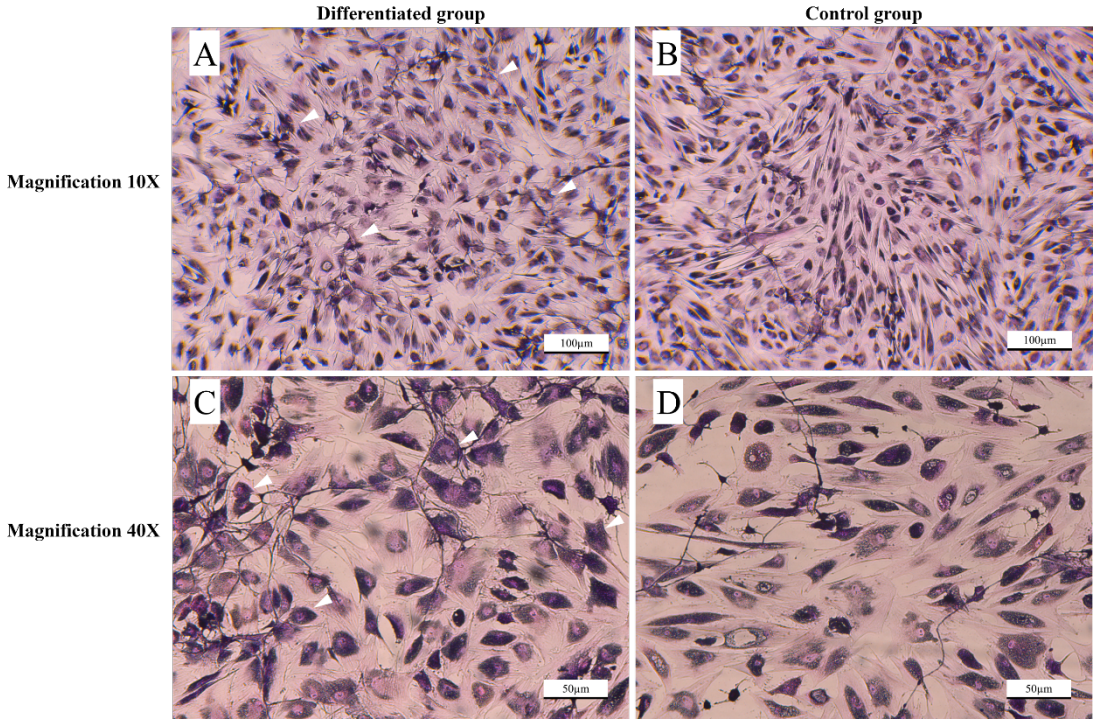

Figure 6 Morphological changes in PTLC-induced feline AM-MSCs (H&E staining) after 21 days of differentiation. The PTLCs-induced group (A and C) displayed a higher density of polygonal-shaped cells (arrowhead) and a lower density of spindle-shaped cells compared to the control group (B and D). A and B: Scale bar = 100 µm. C and D: Scale bar = 50 µm.

Gene expression analysis

The expression levels of three proximal tubular-like cell (PTLC)-related genes, Paired box gene 2 (*PAX2*), Gene Aquaporin 1 (*AQP1*), and Gamma-glutamyltransferase 1 (*GGT*), were evaluated in AM-MSCs following differentiation at days 14 and 21. Their expression was analyzed by RT-qPCR and presented as fold-change relative to the control group (baseline = 1), with values displayed on a log scale (Figure 7).

PAX2 belongs to the family which plays a crucial role in tissue and organ formation during the embryonic stage. The expression of *PAX2* gene directs the synthesis of protein vital for the development of kidneys, urinary tract, and genital tract. In this study, upregulation of *PAX2* was observed in samples 2 and 3 at day 14 post-induction, reaching 2469.4-fold and 18936.6-fold compared to control, whereas sample 1 showed a low induction of of 1.3-fold. By day 21, sample 2 maintained high expression (15,994.5-fold), while sample 3 declined to 107.0-fold. Sample 1 remained at a low level (1.4-fold). The mean expression across samples was 7,135.5 ± 4,202.5 at day 14 and 5,390.1 ± 3,757.2 at day 21 (Figure 7A). Despite variation across samples, no consistent expression trend was observed over time or between conditions (Figure 7A).

AQP1 forms water-specific channels that provide high permeability to water across the plasma membranes of red cells and kidney proximal tubules. *AQP1* exhibits selective membranous expression in renal tubules. At day 14, expression was evaluated acrossall samples (15.7-, 11599.6-, and 8349.8-fold). On day 21, samples 1 and 2 maintained increased levels (21.7- and 14416.2-fold), while sample 3 showed a decrease (666.5-fold) (Figure 7A) The mean values were 6,650.1 ± 2,439.3 at day 14 and 5,028.0 ± 3,319.4 at day 21. Statistical analysis by Mann–Whitney U test revealed no significant differences between the control and induced groups or across time points (Figure 7A).

GGT encodes an enzyme that catalyzes the transfer of the glutamyl moiety of glutathione to various amino acids and dipeptide acceptors. *GGT* gene expression is prominent in the kidney. At day 14, high expression was observed in samples 2 and 3 (825.8- and 196.8-fold), whereas sample 1 remained low (0.4-fold) (Figure 7B). The mean expression was 340.9 ± 176.0 at day 14 and 483.9 ± 341.5 at day 21, with no statistically significant differences between groups or time points (Figure 7A).

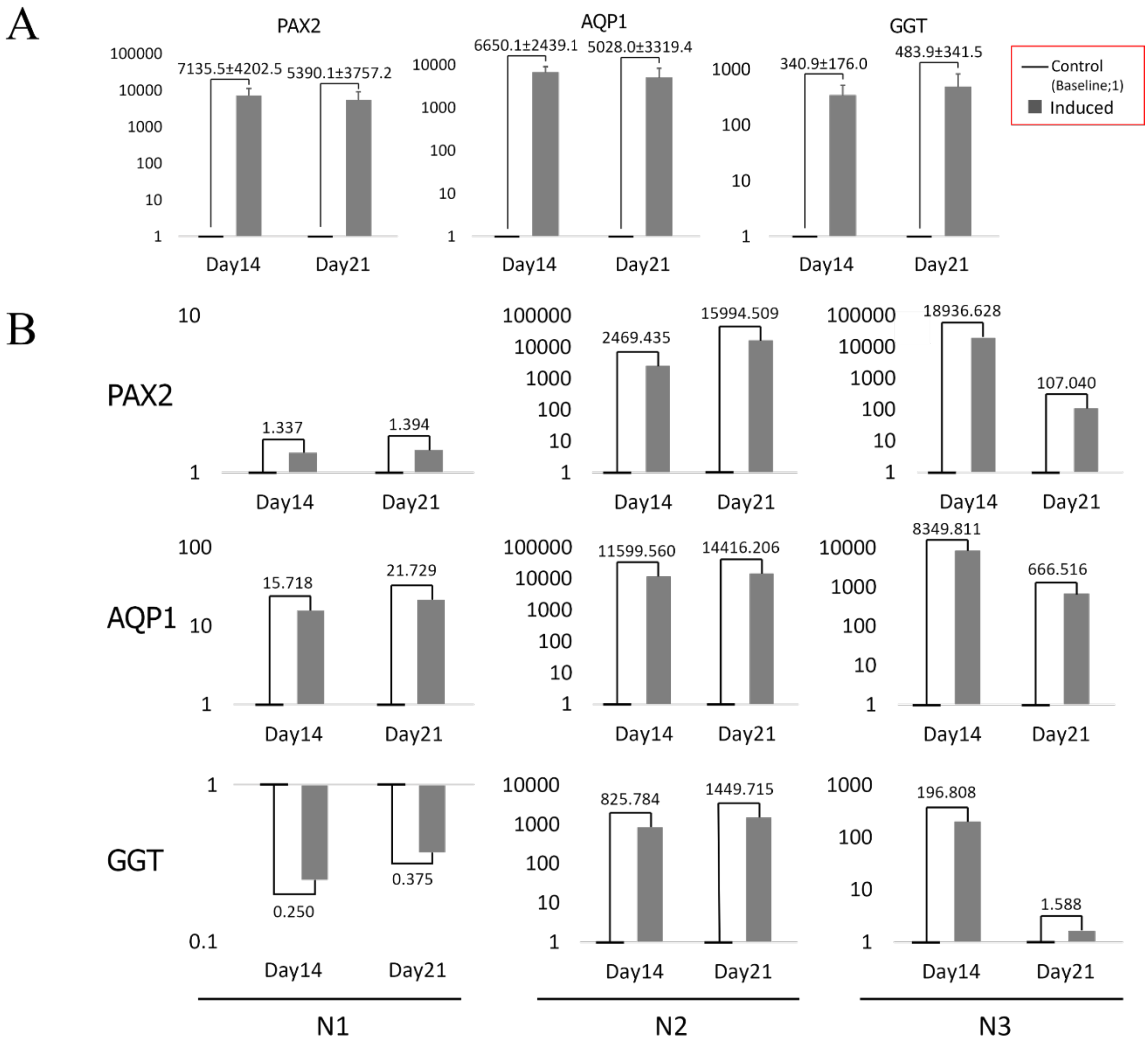

Figure 7 Fold change in gene expression levels of *PAX2, AQP1, and GGT* in PTLC-induced AM-MSCs at days 14 and 21 of culture. (A) Mean ± SEM of relative gene expression levels comparing control and induced group (N = 3) at each time point (B) Individual RT-qPCR expression profiles for each gene in three feline AM-MSCs samples. Grey bars represent the induced (differentiated) group, and black bars represent the control group. The Y-axis displays relative gene expression levels in log transformation, normalized to the control (baseline = 1). in the graph. Samples are labeled N1, N2, and N3.

DISCUSSION

This study presents a successful validation of the isolation protocol for MSCs from feline placentas, achieving a cell survival rate exceeding 80%. This high viability underscores the reliability of the employed method, ensuring minimal

cellular stress during isolation. Morphologically, the isolated cells exhibited the characteristic spindle shape and plastic adherence typical of MSCs, in line with prior observations in humans (Tsujimura et al., 2016; Lukomska et al., 2019), canines (Rashid et al., 2021), and felines (Vidane et al., 2014). Cell proliferation dynamics, assessed through the Alamar Blue assay, revealed a biphasic growth pattern characterized by an initial rapid proliferation phase followed by a deceleration as confluence approached. Remarkably, the absence of a lag phase highlights the cells' adaptability to in vitro culture, a phenomenon similarly noted in canine MSCs (Zhan et al., 2019). A transient reduction in cell proliferation between days 5-7 was observed, likely due to contact inhibition a common occurrence in MSC culture (Zhan et al., 2019; Tucker et al., 2020). Following this brief arrest, the cells resumed steady proliferation until confluence was reached. In general, CD90 is a well-recognized marker for MSCs, typically expressed at high levels (>80%) in MSCs derived from various sources such as bone marrow, adipose tissue, umbilical cord, and amnion tissue (Ambrosio et al., 2020; Rashid et al., 2021; Yang et al., 2023). This finding aligns with the consistently high expression of CD90 (>80%) in our study, further validating the mesenchymal identity of the isolated cells. Beyond CD90, MSCs are characterized by high expression of CD73 and CD105, as specified by the International society for cell and gene therapy (ISCT) (Dominici et al., 2006). Additionally, CD44, commonly found in MSCs from bone marrow and Wharton's Jelly, is essential for cell adhesion and migration (Xu et al., 2020; Primeaux et al., 2022). In this study, CD73 showed moderate expression (40%), whereas the expression of CD44 and CD105 was notably low (<2%), possibly due to tissue origin, species-specific factors, culture-related variability, or suboptimal cross-reactivity of antibodies with feline epitopes (Choi et al., 2014; Adan et al., 2017; Lee et al., 2017). The variability in marker expression, particularly for CD73 and CD44, may also reflect cellular heterogeneity, passage-related changes, or culture conditions. Minimal expression of CD34 and MHC class II further supports the absence of hematopoietic contamination. MHC class I was expressed at a low level, which, along with minimal MHC class II expression, supports the low immunogenic nature of these cells, a favorable feature for allogeneic use. Although cell sorting techniques were not employed in this study, such methods are particularly important in translational or clinical settings, where high cell purity and batch consistency are critical for safety and efficacy. Future work aiming to translate these findings into therapeutic applications should include sorting or clonal expansion to ensure clinical-grade MSC production.

With respect to the stemness characteristics associated with mesodermal lineage differentiation, the isolated AM-MSCs were evaluated under different culturing circumstances. The ability of AM-MSCs to undergo trilineage differentiation was successfully demonstrated, as evidenced by positive staining results for adipogenesis, chondrogenesis, and osteogenesis using Oil Red O, Safranin O, and Alizarin Red S, respectively. This differentiation capability illustrates the cells' potential to transform into mesodermal lineage derivatives, accompanied by notable morphological changes and the production or secretion of extracellular matrix components (Rashid et al., 2021). Specifically, lipid droplet accumulation in adipocytes was detected by Oil Red O staining, proteoglycan deposition in chondrocytes was highlighted by Safranin O staining, and calcium-rich deposits in osteocytes were visualized using Alizarin Red S staining (Chan et al., 2022). These findings reinforce the multipotency of the isolated AM-MSCs, demonstrating their stemness properties.

The differentiation of AM-MSCs into PTLCs was guided by a sequential application of bioactive molecules. Initially, a ROCK inhibitor used to enhance cell survival and prime lineage commitment (Lindstrom et al., 2013). Subsequently, BMP2 and BMP7 were introduced to mimic nephrogenic cues observed during kidney development (Godin et al., 1999; Tsujimura et al., 2016). Insulin was added to stimulate the expression of water transport proteins, a hallmark of proximal

tubular function (Flyvbjerg et al., 2004; Bach and Hale, 2015). Finally, TGF-beta was included to promote activin release, facilitating tubular differentiation (Loomans and Andl, 2014; Abarca-Buis et al., 2021; de Ruiter et al., 2023). Morphologically, the induced cells transformed into polygonal shapes with rounded nuclei, consistent with previous studies on renal differentiation (Chandrasekaran et al., 2021) (Singaravelu and Padanilam, 2009). During the differentiation process, a transient decrease in cell density was observed, which aligns with the findings of Chandrasekaran, V., et al. (Chandrasekaran et al., 2021). This temporary reduction in density may be attributed to the combined effects of ROCK inhibitor-induced suppression of cell proliferation and the pleiotropic actions of TGF-beta on cell cycle regulation (Abarca-Buis et al., 2021).

Gene expression analysis of nephron-associated markers (*PAX2*, *AQP1*, and *GGT*) revealed no statistically significant differences between PTLC-induced AM-MSCs and control groups or across time points, as determined by the Mann–Whitney U test ($p > 0.05$). However, descriptive trends suggest successful initiation of renal-like differentiation. Specifically, *PAX2* and *AQP1* were markedly upregulated in samples 2 and 3, particularly at day 14, with varying expression patterns by day 21. *GGT* also followed this trend, though with less consistency Sample 1 demonstrated minimal induction across all three genes. These findings suggest that feline AM-MSCs possess the capacity to differentiate into PTLC-like cells, albeit with donor-dependent variability—a well-documented phenomenon in MSC research (Ramakrishnan et al., 2014).

Notably, *PAX2* plays a key role in early nephrogenesis, guiding kidney and urinary tract development, while *AQP1* and *GGT* serve as functional markers for proximal tubular cells by mediating water transport and glutathione metabolism, respectively (Singaravelu and Padanilam, 2009). In this study, their expression patterns, particularly the early surge of *PAX2* followed by sustained or reduced *AQP1* and *GGT* levels, may reflect temporal dynamics in PTLC differentiation. This biological heterogeneity, possibly influenced by donor variability or subtle differences in induction responsiveness, highlights the complexity of MSC differentiation outcomes. It also underscores the importance of species-specific gene regulation and potential limitations in primer efficiency across feline samples (Romero et al., 2012; Brown and Turner, 2021).

Future studies should focus on protocol refinement and large-scale validation to enhance reproducibility and minimize inter-donor variation. Additionally, addressing species-specific regulatory mechanisms and optimizing primer design will be crucial for improving accuracy in feline PTLC differentiation studies. While this study use a 2D induction system, gene expression patterns suggest a transition toward renal lineage commitment, albeit not to full maturation. Further validation using immunohistochemical and ultrastructural analysis (e.g., brush border formation) is recommended. These results provide a foundation step toward the therapeutic application of feline AM-MSCs in renal tubular regeneration. Importantly, they are consistent with previous studies demonstrating the safety of autologous adipose-derived MSCs transplantation (Thomson et al., 2019), and improved renal function following allogeneic MSC administration (Zacharias et al., 2021).

CONCLUSIONS

In summary, this study underscores the potential of feline AM-MSCs for differentiation into PTLCs, paving the way for innovative regenerative therapies targeting feline CKD. To translate these findings into clinical applications, future research should focus on optimizing the differentiation protocol to minimize variability, employing fluorescence imaging and 3D culture for enhanced validation, and conducting in vivo transplantation studies to assess long-term efficacy. These

efforts will be instrumental in advancing stem cell-based therapies for feline renal diseases and may also extend their applicability to other species.

ACKNOWLEDGEMENTS

The authors would like to acknowledge the Small Animal Hospital, Faculty of Veterinary Medicine, and the Department of Anatomy, Faculty of Medicine, Chiangmai University, for supporting and allowing the use of laboratory facilities in this project.

AUTHORS' CONTRIBUTIONS

Pachara Pornnimitara: Conceptualization (lead); methodology (equal); investigation (equal); data analysis (equal); writing – original draft (lead); formal analysis (lead); project administration (equal).
Wanna Suriyasathaporn: Conceptualization (supporting); investigation (equal); writing – review and editing (equal); supervision (equal); project administration (equal); funding acquisition (equal).
Kantirat Yaja: Methodology (equal); validation (equal).
Suteera Narakornsak: Conceptualization (supporting); methodology (equal); validation (equal); investigation (equal); data analysis (equal); writing – review and editing (equal); supervision (equal); funding acquisition (equal).
Sasithorn Panasophonkul: Conceptualization (supporting); methodology (equal); validation (equal); investigation (equal); data analysis (equal); writing – review and editing (equal); supervision (equal); funding acquisition (equal).

REFERENCES

Abarca-Buis, R.F., Mandujano-Tinoco, E.A., Cabrera-Wrooman, A., Krotzsch, E., 2021. The complexity of TGFbeta/activin signaling in regeneration. J. Cell Commun. Signal. 15, 7-23.

Adan, A., Alizada, G., Kiraz, Y., Baran, Y., Nalbant, A., 2017. Flow cytometry: basic principles and applications. Crit. Rev. Biotechnol. 37, 163-176.

Ambrosio, C.E., Orlandin, J.R., Oliveira, V.C., Motta, L.C.B., Pinto, P.A.F., Pereira, V.M., Padoveze, L.R., Karam, R.G., Pinheiro, A.O., 2020. Potential application of aminiotic stem cells in veterinary medicine. Anim. Reprod. 16, 24-30.

Aronson, L.R., 2016. Update on the current status of kidney transplantation for chronic kidney disease in animals. Vet. Clin. North Am. Small Anim. Pract. 46, 1193-1218.

Bach, L.A., Hale, L.J., 2015. Insulin-like growth factors and kidney disease. Am. J. Kidney Dis. 65, 327-336.

Chan, Y.H., Ho, K.N., Lee, Y.C., Chou, M.J., Lew, W.Z., Huang, H.M., Lai, P.C., Feng, S.W., 2022. Melatonin enhances osteogenic differentiation of dental pulp mesenchymal stem cells by regulating MAPK pathways and promotes the efficiency of bone regeneration in calvarial bone defects. Stem Cell Res. Ther. 13, 73.

Chandrasekaran, V., Carta, G., da Costa Pereira, D., Gupta, R., Murphy, C., Feifel, E., Kern, G., Lechner, J., Cavallo, A.L., Gupta, S., Caiment, F., Kleinjans, J.C.S., Gstraunthaler, G., Jennings, P., Wilmes, A., 2021. Generation and characterization of iPSC-derived renal proximal tubule-like cells with extended stability. Sci. Rep. 11, 11575.

Choi, E.W., et, al., 2014. Feline mesenchymal stem cells derived from amniotic fluid and their potential for differentiation. J. Vet. Sci. 15, 515–522.

Cianci, R., Simeoni, M., Cianci, E., De Marco, O., Pisani, A., Ferri, C., Gigante, A., 2023. Stem cells in kidney ischemia: from inflammation and fibrosis to renal tissue regeneration. Int. J. Mol. Sci. 24, 4631.

de Ruiter, R.D., Wisse, L.E., Schoenmaker, T., Yaqub, M., Sanchez-Duffhues, G., Eekhoff, E.M.W., Micha, D., 2023. TGF-Beta induces activin A production in dermal fibroblasts derived from patients with Fibrodysplasia ossificans progressiva. Int. J. Mol. Sci. 24, 2299.

Dominici, M., Le Blanc, K., Mueller, I., Slaper-Cortenbach, I., Marini, F., Krause, D., Deans, R., Keating, A., Prockop, D., Horwitz, E., 2006. Minimal criteria for defining multipotent mesenchymal stromal cells. The International Society for Cellular Therapy position statement. Cytotherapy. 8, 315-317.

Flyvbjerg, A., Khatir, D.S., Jensen, L.J., Dagnaes-Hansen, F., Gronbaek, H., Rasch, R., 2004. The involvement of growth hormone (GH), insulin-like growth factors (IGFs) and vascular endothelial growth factor (VEGF) in diabetic kidney disease. Curr. Pharm. Des. 10, 3385-3394.

Godin, R.E., Robertson, E.J., Dudley, A.T., 1999. Role of BMP family members during kidney development. Int. J. Dev. Biol. 43, 405-411.

Hass, R., Kasper, C., Bohm, S., Jacobs, R., 2011. Different populations and sources of human mesenchymal stem cells (MSC): A comparison of adult and neonatal tissue-derived MSC. Cell Commun. Signal. 9, 12.

Hsu, R.K., Hsu, C.Y., 2016. The role of acute kidney injury in chronic kidney disease. Semin. Nephrol. 36, 283-292.

Kim, K.M., Oh, H.J., Choi, H.Y., Lee, H., Ryu, D.R., 2019. Impact of chronic kidney disease on mortality: A nationwide cohort study. Kidney Res. Clin. Pract. 38, 382-390.

Lee, Y., et, al., 2017. Characterization and multilineage differentiation of feline amniotic mesenchymal stem cells. Tissue Engineering and Regenerative Medicine 14, 681-692.

Lindstrom, N.O., Hohenstein, P., Davies, J.A., 2013. Nephrons require Rho-kinase for proximal-distal polarity development. Sci. Rep. 3, 2692.

Loomans, H.A., Andl, C.D., 2014. Intertwining of activin A and TGFbeta signaling: dual roles in cancer progression and cancer cell invasion. Cancers (Basel). 7, 70-91.

Lukomska, B., Stanaszek, L., Zuba-Surma, E., Legosz, P., Sarzynska, S., Drela, K., 2019. Challenges and controversies in human mesenchymal stem cell therapy. Stem. Cells. Int. 2019, 9628536.

Noh, S.A., Kim, T., Ju, J., 2021. Case reports of amniotic membrane derived-cell treatment for feline chronic renal failure. J. Anim. Reprod. Biotechnol. 36, 116-120.

Perini-Perera, S., Del-Angel-Caraza, J., Perez-Sanchez, A.P., Quijano-Hernandez, I.A., Recillas-Morales, S., 2021. Evaluation of chronic kidney disease progression in dogs with therapeutic management of risk factors. Front. Vet. Sci. 8, 621084.

Piyarungsri, K., Tangtrongsup, S., Thongtharb, A., Sodarat, C., Bussayapalakorn, K., 2020. The risk factors of having infected feline leukemia virus or feline immunodeficiency virus for feline naturally occurring chronic kidney disease. Vet. Integr. Sci. 18, 119-131.

Primeaux, M., Gowrikumar, S., Dhawan, P., 2022. Role of CD44 isoforms in epithelial-mesenchymal plasticity and metastasis. Clin. Exp. Metastasis. 39, 391-406.

Ramakrishnan, A., Torok-Storb B Fau - Pillai, M.M., Pillai, M.M., 2014. Primary marrow-derived stromal cells: isolation and manipulation. Methods Mol. Biol. 1035, 75–101.

Rashid, U., Yousaf, A., Yaqoob, M., Saba, E., Moaeen-Ud-Din, M., Waseem, S., Becker, S.K., Sponder, G., Aschenbach, J.R., Sandhu, M.A., 2021. Characterization and differentiation potential of mesenchymal stem cells isolated from multiple canine adipose tissue sources. BMC Vet. Res. 17, 388.

Singaravelu, K., Padanilam, B.J., 2009. In vitro differentiation of MSC into cells with a renal tubular epithelial-like phenotype. Ren. Fail. 31, 492-502.

Sobhani, A., Khanlarkhani, N., Baazm, M., Mohammadzadeh, F., Najafi, A., Mehdinejadiani, S., Sargolzaei Aval, F., 2017. Multipotent stem cell and current application. Acta Med. Iran. 55, 6-23.

Thomson, A.L., Berent, A.C., Weisse, C., Langston, C.E., 2019. Intra-arterial renal infusion of autologous mesenchymal stem cells for treatment of chronic kidney disease in cats: Phase I clinical trial. J. Vet. Intern. Med. 33, 1353-1361.

Thornton, C., 2017. Supporting quality of life in feline patients with chronic kidney disease. Vet. Nurs. 8, 200-206.

Tsujimura, T., Idei, M., Yoshikawa, M., Takase, O., Hishikawa, K., 2016. Roles and regulation of bone morphogenetic protein-7 in kidney development and diseases. World J. Stem. Cells. 8, 288-296.

Tucker, D., Still, K., Blom, A., Hollander, A., Kafienah, W., 2020. Over-confluence of expanded bone marrow mesenchymal stem cells ameliorates their chondrogenic capacity in 3D cartilage tissue engineering. Available online: https://www.biorxiv.org/content/10.1101/2020.01.08.897645v1.full

Vidane, A.S., Souza, A.F., Sampaio, R.V., Bressan, F.F., Pieri, N.C., Martins, D.S., Meirelles, F.V., Miglino, M.A., Ambrosio, C.E., 2014. Cat amniotic membrane multipotent cells are nontumorigenic and are safe for use in cell transplantation. Stem Cells Cloning. Adv. Appl. 7, 71-78.

Westenfelder, C., Togel, F.E., 2011. Protective actions of administered mesenchymal stem cells in acute kidney injury: relevance to clinical trials. Kidney Int. Suppl. 1, 103-106.

Xu, Y., Wang, Y.Q., Wang, A.T., Yu, C.Y., Luo, Y., Liu, R.M., Zhao, Y.J., Xiao, J.H., 2020. Effect of CD44 on differentiation of human amniotic mesenchymal stem cells into chondrocytes via Smad and ERK signaling pathways. Mol. Med. Rep. 21, 2357-2366.

Yang, H., Chen, J., Li, J., 2023. Isolation, culture, and delivery considerations for the use of mesenchymal stem cells in potential therapies for acute liver failure. Front. Immunol. 14, 1243220.

Zacharias, S., Welty, M.B., Sand, T.T., Black, L.L., 2021. Impact of allogeneic feline uterine-derived mesenchymal stromal cell intravenous treatment on renal function of nephrectomized cats with chronic kidney disease. Res. Vet. Sci. 141, 33-41.

Zhan, X.S., El-Ashram, S., Luo, D.Z., Luo, H.N., Wang, B.Y., Chen, S.F., Bai, Y.S., Chen, Z.S., Liu, C.Y., Ji, H.Q., 2019. A comparative study of biological characteristics and transcriptome profiles of mesenchymal stem cells from different canine tissues. Int. J. Mol. Sci. 20, 1485.

How to cite this article;
Pachara Pornnimitara, Wanna Suriyasathaporn, Kantirat Yaja, Suteera Narakornsak and Sasithorn Panasophonkul. *In vitro* differentiation of feline amniotic-derived mesenchymal stem cells into proximal tubular-like cells: A pilot study. Veterinary Integrative Sciences. 2026; 24(1): e2026025-1-18.